Effect of Observer Experience in the Differentiation Between Benign and Malignant Liver Tumors After Ultrasound Contrast Agent Injection

Emilio Quaia, MD, Valerio Alaimo, MD, Elisa Baratella, MD, Riccardo Pizzolato, MD, Giacomo Cester, MD, Alessandro Medeot, MD, Maria Assunta Cova, MD

Objective. The purpose of this study was to assess the impact of the observer level of experience on the diagnostic performance of contrast-enhanced ultrasound imaging (CEUS) for differentiation between benign and malignant liver tumors. ***Methods.*** From a computerized search, we retrospectively identified 286 biopsy-proven liver tumors (105 hepatocellular carcinomas, 48 metastases, 7 intrahepatic cholangiocarcinomas, 33 liver hemangiomas, and 93 nonhemangiomatous benign lesions) in 235 patients (140 male and 95 female; mean age ± SD, 56 ± 11 years) who underwent CEUS after sulfur hexafluoride-filled microbubble injection. The digital cine clips recorded during the arterial (10–35 seconds from injection), portal (50–120 seconds), and late (130–300 seconds) phases were analyzed by 6 independent observers without experience (group 1, observers 1–3) or with 2 to 10 years of experience in CEUS (group 2, observers 4–6). Specific training in the diagnostic and interpretative criteria was provided to the inexperienced observers. Each observer used a 5-point scale to grade diagnostic confidence: 1, definitely benign; 2, probably benign; 3, indeterminate; 4, probably malignant; or 5, definitely malignant on the basis of the enhancement pattern during the arterial phase and enhancement degree during the portal and late phases compared with the liver (hypoenhancement indicating malignant and isoenhancement to hyperenhancement indicating benign). ***Results.*** The analysis of observer diagnostic confidence revealed higher intragroup (κ = 0.63–0.83) than intergroup (κ = 0.47–0.63) observer agreement. The experienced observers showed higher diagnostic performance in malignancy diagnosis than did inexperienced observers (overall accuracy: group 1, 63.3%–72.8%; group 2, 75.9%–93.1%; $P < .05$, χ^2 test). ***Conclusions.*** The diagnostic performance of CEUS in liver tumor characterization was dependant on the observer's level of experience. ***Key words:*** contrast-enhanced ultrasound imaging; liver; microbubbles; tumor.

Abbreviations
CEUS, contrast-enhanced ultrasound imaging; CT, computed tomography; MRI, magnetic resonance imaging

Received April 23, 2009, from the Department of Radiology, Cattinara Hospital, University of Trieste, Trieste, Italy (E.Q., E.B., R.P., G.C., A.M., M.A.C.); and Department of Radiology, University of Palermo, Palermo, Italy (V.A.). Revision requested June 4, 2009. Revised manuscript accepted for publication August 13, 2009.

We thank Lucio Torelli, associate professor of statistics, Department of Mathematics, University of Trieste, who gave important suggestions for the statistical analysis and data presentation.

Address correspondence to Emilio Quaia, MD, Department of Radiology, Cattinara Hospital, University of Trieste, Strada di Fiume 447, 34149 Trieste, Italy.

E-mail: equaia@yahoo.com

Gray scale and color Doppler ultrasound imaging are limited in characterizing liver tumors because of the similar appearance and vascular architecture of malignant and benign lesions.[1,2] Contrast-enhanced ultrasound imaging (CEUS)[3–5] has been shown to overcome the limitations of unenhanced ultrasound imaging and allows a definite improvement in liver tumor characterization.[6–12] Ultrasound contrast agents are microbubbles presenting a pure intravascular distribution, even though some agents, including SH U 508A (Levovist; Schering AG, Berlin, Germany) and perfluorobutane (Sonazoid; GE Healthcare, Chalfont St Giles, England), present a postvascular hepato-specific phase from 2 to 5 minutes after intravenous injection. This phe-

nomenon is probably determined by the adherence of the microbubbles to the hepatic sinusoids or by selective uptake by the phagocytic cells of the reticuloendothelial system. Because ultrasound contrast agents do not leak in the interstitial space but persist in the sinusoids and portal vessels,[4,5] no equilibrium phase exists, and enhancement of the liver parenchyma shows progressive decay until the baseline appearance is again observed. The enhancement resulting exclusively from the hepatic arterial supply is timed from 10 to 20 seconds after intravenous contrast agent injection and lasts for 10 to 15 seconds.[13,14] The portal phase lasts until 2 minutes after contrast agent injection, whereas the late phase lasts up to 4 to 6 minutes after injection until microbubble clearance from the liver parenchyma.[13,14]

The tumor enhancement pattern during the arterial phase, namely, the distribution of the increased echo signal intensity after ultrasound contrast agent injection within the lesion, provides a valuable clue to the benign or malignant nature of the lesion. Many different enhancement patterns have been described,[6–12] some more common in malignancies (peripheral rimlike enhancement in metastases[15]), some typically identified in benign lesions (peripheral nodular enhancement in hemangiomas[16] and a central spoked wheel-shaped enhancement in focal nodular hyperplasia[17]), and others common both to malignant and benign liver tumors (diffuse enhancement in hepatocellular carcinomas,[15] adenomas, and focal nodular hyperplasia[17] and absence of enhancement in metastases and avascular thrombotic hemangiomas[16]). However, the enhancement patterns observed during the arterial phase are not sufficient for characterizing liver tumors.[18] The evaluation of the degree of tumor enhancement during the portal and late phases, namely, the grade of tumoral echo signal intensity compared with the liver parenchyma, is essential for the final diagnosis because malignant tumors prevalently show a hypoenhancing appearance, whereas benign tumors tend to show an isoenhancing or a hyperenhancing appearance due to persistent ultrasound contrast agent uptake.[18] Frequently, the degree of tumor enhancement changes from the portal to late phase, and this could potentially influence the final diagnosis according to the observer's visual evaluation and level of experience. To our knowledge, no previous study has analyzed how the observer experience in the interpretation of the tumor enhancement pattern and degree after microbubble injection could influence the diagnostic performance in liver tumor characterization.

The objective of this study was to assess the impact of the observer level of experience on the diagnostic performance of CEUS for differentiation between benign and malignant liver tumors.

Materials and Methods

Patients

Approval for this retrospective study was granted by the Ethics Review Board of our hospital, and informed consent was obtained from all patients at the time of scanning after the nature of the procedure had been fully explained.

From a computerized search of our hospital's database of radiologic records from January 2004 to January 2008, a reference radiologist responsible for the study identified 390 consecutive patients (235 male and 155 female; mean age ± SD, 57 ± 13 years) with 440 liver tumors studied by CEUS after sulfur hexafluoride-filled microbubble (SonoVue, Bracco SpA, Milan, Italy) injection. Liver tumors had been detected by gray scale ultrasound imaging or cross-sectional imaging (multiphase contrast-enhanced computed tomography [CT] or magnetic resonance imaging [MRI]) and corresponded to incidental liver tumors discovered during a routine clinical diagnostic workup (n = 225) or suspected malignancies identified during staging before surgery or postsurgical follow-up (n = 105) or surveillance for chronic liver disease (n = 110). To complete the diagnostic workup, those tumors detected only by gray scale ultrasound imaging were scanned by multiphase cross-sectional imaging techniques (CT, MRI, or both) 2 to 15 days after detection.

All liver tumors were then studied by CEUS 1 to 28 days after detection because they were considered indeterminate at the time of diagnosis by the on-site radiologists, who had 10 to 20 years of experience in abdominal radiology. Indeterminate liver tumors were those that did not reveal any

definite features with regard to the nature (benign or malignant) or histotype and those in which unenhanced gray scale ultrasound imaging with color or power Doppler or cross-sectional imaging were inconclusive. Up to 2 lesions per patient were selected for CEUS on the basis of largest diameter and best visualization through the acoustic window according to the on-site radiologist's evaluation. Ultrasound-guided core needle biopsy was performed with 18- to 20-gauge modified Menghini needles 2 to 15 days after CEUS, and the histologic findings were considered the reference standards for the final diagnoses.

The reference radiologist excluded 154 liver tumors because of technical inadequacy of the CEUS due to failure in data storage (n = 5), incomplete tumor visibility (n = 25), or lack of a histologic diagnosis due to the typical malignant pattern depicted by CEUS, CT, or MRI (n = 110)—evidence of multiple additional enhancing lesions with a hypoenhancing appearance during the portal and late phases or tumors greater than 5 cm in diameter with heterogeneous contrast enhancement during the arterial phase and a hypoenhancing appearance during the portal and late phases; and a high probability of liver hemangiomas (n = 14)—evidence of obvious peripheral nodular enhancement (discontinuous or continuous peripheral nodular appearance) with centripetal fill-in. Therefore, 286 liver tumors (Table 1) in 235 patients (mean age ± SD, 56 ± 11 years; median, 58 years; range, 40–75 years), 140 male (mean age, 55 ± 11 years; median, 58 years; range, 45–75 years) and 95 female (mean age, 56 ± 10 years; median, 57 years; range, 40–65 years), were finally included in the study. The difference in the median age between male and female patients was not found to be statistically significant ($P > .05$, Mann-Whitney nonparametric U test, applied after a Shapiro-Wilk test failed to show a normal distribution of age data).

Contrast-Enhanced Ultrasound Examinations

All examinations were performed on the same system (Acuson Sequoia; Siemens Medical Solutions, Mountain View, CA; with a convex array 2- to 4-MHz 4C1 transducer) by on-site radiologists. Before microbubble injection, the liver tumors were assigned a liver segment location[19,20]; the tumor diameter was measured in the transverse and longitudinal planes with calipers, and the largest diameter in centimeters was recorded.

Microbubbles were then manually injected as a 2.4-mL bolus through an 18- to 20-gauge intravenous cannula followed by a 10-mL normal saline flush, and each tumor was scanned by real-time continuous insonation during normal

Table 1. General Features of Different Histotypes

Histotype	n	Mean Size ± SD, cm	Size Range, cm
Hepatocellular carcinomas[a]	105	2.5 ± 1.6	2–4.2
Metastases[b]	48	3.1 ± 0.9	1–5
Intrahepatic cholangiocarcinomas	7	2.5 ± 1.6	1.9–4.7
Hemangiomas[c]	33	1.9 ± 0.6	1–3.5
Focal nodular hyperplasia	30	1.9 ± 0.6	1–4.5
Hepatocellular adenomas	15	3.5 ± 1.4	1–5
Regenerative nodules[d]	19	1.9 ± 0.8	1–4.2
Focal fatty sparing/changes	25	1.9 ± 0.6	0.8–3
Other benign histotypes[e]	4	3.7 ± 1.2	2–5
Total	286	2.3 ± 1.1	1–5

Dimensions are expressed to 1 decimal place because of the relatively small size of many tumors and refer to the largest diameter of each tumor.
[a]Hepatocellular carcinomas revealed a well-differentiated (n = 65), moderately differentiated (n = 28), or poorly differentiated (n = 12) pattern on a background of liver cirrhosis.
[b]Liver metastases were found in patients with colorectal (n = 35), gastric (n = 5), or pancreatic (n = 3) adenocarcinomas or breast (n = 3) or renal cell (n = 2) carcinomas.
[c]Liver hemangiomas revealed endothelium-lined vascular channels (n = 6) or a hypervascular (n = 21) or thrombotic-fibrotic (n = 6) pattern at histologic analysis.
[d]Regenerative nodules were well-differentiated (n = 14), low-grade (n = 3), or high-grade (n = 2) dysplastic nodules.
[e]Included 1 necrotic nodule (2 cm in diameter), 1 intrahepatic extramedullary hematopoiesis (4 cm), and 2 liver abscesses (4 and 5 cm).

breathing or breath holding, depending on which yielded the best visualization of the tumor. Technical parameters were as follows: Cadence contrast pulse sequencing as a contrast-specific technique; tissue equalization applied before contrast agent injection; echo signal gain below noise visibility; low transmit power (mechanical index, 0.14–0.16), dynamic range, 75 dB; temporal resolution between frames, 75 to 100 milliseconds (10–13 frames per second); signal persistence turned off; and 2 focal zones below the level of the tumor. The arterial phase was timed for 10 to 35 seconds after microbubble injection, the portal venous phase for 50 to 120 seconds, and the late phase for 130 to 300 seconds.[12,13]

Distinct digital cine clips for the arterial, portal venous, and late phases of the CEUS study were stored on a personal computer (Pentium 4; Intel Corporation, Santa Clara, CA) connected to the ultrasound equipment by means of frame-grabber software (Mediacruise; Canopus Corporation, San Jose, CA) with an integrated high-performance hardware-based real-time Moving Picture Experts Group 2 encoder (Mediacruise MVR1000). Digital cine clips had a duration of 10 to 20 seconds during the arterial phase, 40 to 50 seconds during the portal phase, and 100 to 120 seconds during the late phase.

Cine Clip Analysis

The digital cine clips stored on DVDs were retrospectively reviewed by 6 observers who were affiliated with the hospital in which the study was performed and were not involved in patient scanning. The first 3 observers (group 1, observers 1–3) were 2 chief residents and 1 board-certified radiologist who had 1, 3, and 8 years of experience in abdominal ultrasound imaging, respectively, but no experience in CEUS. The other 3 observers (group 2, observers 4–6) were board-certified radiologists who had 2, 5, and 10 years of experience in CEUS performed at least twice a week. Specific training in the diagnostic and interpretative criteria used in this study was provided by the reference radiologist responsible for the study to the inexperienced observers, who reviewed 15 to 20 cases before the beginning of the independent cine clip interpretation. Training cine clips included benign and malignant liver tumors presenting all possible enhancement patterns. Exclusively for the specific training period, the final diagnosis proposed by each inexperienced observer was confirmed or not by the reference radiologist, who made the reader aware of the final diagnosis.

All observers worked independently and were blinded to the identification, clinical history, biopsy results, and other imaging findings of the patients. Digital cine clips of each lesion were randomly assigned to each observer, and all readings were performed on the same computer (Intel Pentium 4 with a 19-in [48-cm] thin-film transistor display) at a central location with Power-DVD software (CyberLink Corporation, Fremont, CA). Each observer was presented with digital cine clips recorded during the arterial, portal, and late phases and was asked to assess the tumor enhancement pattern during the arterial phase[6–12] and the degree of tumor enhancement during the different dynamic phases.[11,13,14,18] The enhancement pattern referred to the distribution of the increased echo signal intensity within the lesion, whereas the degree of tumor enhancement referred to the tumoral echo signal intensity compared with the adjacent liver parenchyma after microbubble injection.

Enhancement patterns during the arterial phase were classified as absent (no difference before and after microbubble injection), dotted (tiny separate spots of enhancement distributed throughout the lesion), peripheral nodular (discontinuous or continuous peripheral enhancement with a nodular appearance), peripheral rimlike (a peripheral continuous enhancing rim that demarcated the tumor from the surrounding liver parenchyma), central (involving the central portion of the tumor, defined as spoked wheel shaped if the central vessel appeared to branch toward the tumor periphery), and diffuse (homogeneous or heterogeneous, involving the whole tumor).

Subsequently, each observer assessed the degree of tumor enhancement and visually compared the echo signal intensity of the enhancing intratumoral region(s) with a homogeneous region of the surrounding liver during the different dynamic phases. Figures 1–5 show the classification criteria of tumor enhancement, which was graded according to a 5-grade visual scoring system: +2 or +1 (echo signal intensity much or

slightly higher than that of the liver), 0 (echo signal intensity equal to that of the liver), and –1 or –2 (echo signal intensity slightly or much lower than that of the liver). The arterial phase was analyzed separately because it is related to the arterial perfusion of the lesion, and tumors with absent or peripheral rimlike enhancement were considered hypoenhancing, whereas tumors with central or diffuse enhancement were defined as hyperenhancing or isoenhancing according to the level of echo signal intensity compared with the surrounding liver. Because the degree of tumor enhancement frequently changes after the arterial phase, the portal and late phases were analyzed in combination, and the late phase was considered the reference for grading tumoral vascularity. Liver tumors appearing hypoenhanced, isoenhanced, or hyperenhanced during the portal phase and hypoenhanced during the late phase were classified as hypoenhancing, whereas tumors appearing hypoenhanced, isoenhanced, or hyperenhanced during the portal phase and isoenhanced or hyperenhanced during the late phase were considered isoenhancing or hyperenhancing, respec-

Figure 1. Tumor enhancement degree scored as +2 in a 60-year-old woman with liver metastasis (arrow) scanned 25 seconds after ultrasound contrast agent injection during the arterial phase. The tumor has a hyperenhancing appearance with an echo signal intensity much higher (more than double) that that of the adjacent liver (L), which reveals an intensity similar to that at the baseline.

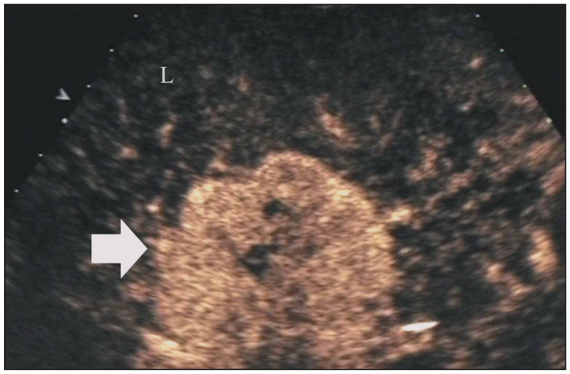

Figure 2. Tumor enhancement degree scored as +1 in a 40-year-old man with focal nodular hyperplasia (arrow) scanned 60 seconds after ultrasound contrast agent injection during the portal phase. The tumor has a hyperenhancing appearance with an echo signal intensity slightly higher (less than double) than that of the adjacent liver.

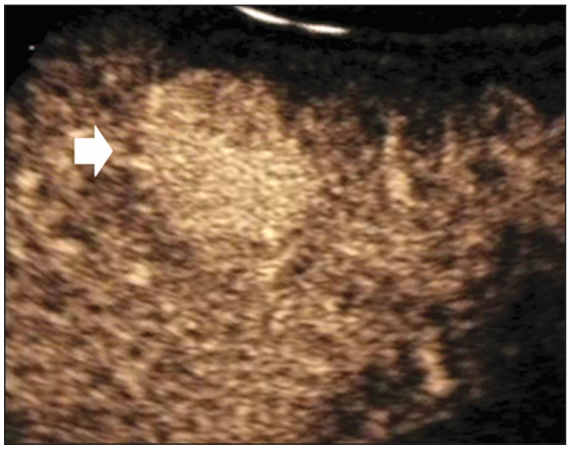

Figure 3. Tumor enhancement degree scored as 0 in a 45-year-old woman with hemangiomas (arrow) scanned 70 seconds after ultrasound contrast agent injection during the portal phase. The tumor has an isoenhancing appearance with an echo signal intensity equal to that of the adjacent liver.

Figure 4. Tumor enhancement degree scored as –1 in a 61-year-old woman with liver cirrhosis and a poorly differentiated hepatocellular carcinoma (arrow) scanned 80 seconds after ultrasound contrast agent injection during the portal phase. The tumor has a hypoenhancing appearance with an echo signal intensity slightly lower (less than half) than that of the adjacent liver.

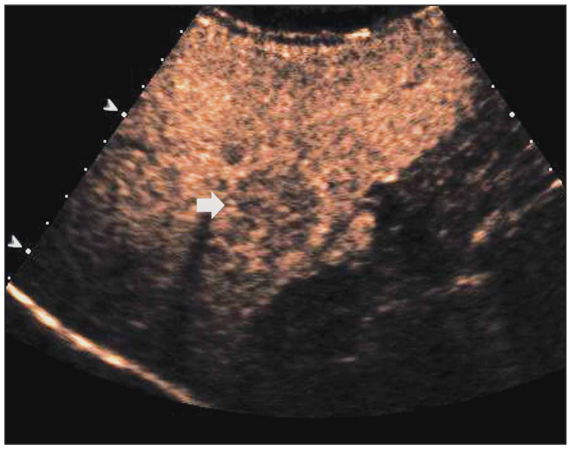

tively. If there was evidence of peripheral rimlike enhancement or incomplete fill-in during the portal and late phases, the tumor was classified as hypoenhancing. The enhancement pattern during the arterial phase and the enhancement degree during the portal and late phases were considered absolute for liver tumor characterization (hypoenhancement during the portal and late phases indicating malignant and isoenhancement to hyperenhancement indicating benign, as described previously[6–17]).

Afterward, the 3 scan sequences (arterial, portal, and late phases) for any given lesion were reviewed in one sitting, and the observers were free to review the digital cine clips as many times as they wished. The cases were interpreted in a set order, and 70 to 80 liver tumors were analyzed in each review session. Six reading sessions separated by a mean of 3 days were necessary to complete the review of all patient scans.

The observers used a 5-point scale to grade diagnostic confidence: 1, definitely benign (evidence of an enhancement pattern typical of benignancy, including central enhancement with a spoked wheel appearance and isoenhancement or hyperenhancement during the portal and late phases); 2, probably benign (diffuse enhancement and isoenhancement or hyperenhancement during the portal and late phases); 3, indeterminate (absent or dotted enhancement and persistent hypoenhancement with or without evidence of peripheral rimlike enhancement); 4, probably malignant; or 5, definitely malignant (absent or dotted enhancement or diffuse homogeneous or heterogeneous enhancement and hypoenhancement during the portal and late phases). Readers had to complete a form with specific multiple-choice questions regarding the tumor enhancement pattern and degree and the diagnostic confidence score. At the conclusion of the review analysis, the reference radiologist transferred all data to Excel spreadsheets (Microsoft Corporation, Redmond, WA) for analysis.

Figure 5. Tumor enhancement degree scored as –2 in a 60-year-old man with a poorly differentiated hepatocellular carcinoma (arrow) scanned 135 seconds after ultrasound contrast agent injection during the late phase. The tumor has a hypoenhancing appearance with a gray scale intensity much lower that of the adjacent liver.

Statistical Analyses

Statistical analyses were performed by using a software package (Analyse-It version 1.63; Analyse-It Software, Leeds, England). The Mann-Whitney *U* test was used to test the differences between malignant and benign tumors in the median visual vascularity score values. The weighted κ statistic was calculated to assess intragroup and intergroup observer agreement.[21] Agreement was graded as poor ($\kappa < 0.20$), fair ($\kappa \geq 0.20$ and < 0.40), moderate ($\kappa \geq 0.40$ and < 0.60), good ($\kappa \geq 0.60$ and < 0.80), and very good ($\kappa \geq 0.8$ up to 1).

The difference in the observers' performance in correctly diagnosing malignancy was calculated by using the χ^2 test with the Yates correction. True-positive cases were tumors correctly assessed as malignant; false-negative cases were tumors incorrectly assessed as benign; true-negative cases were tumors correctly assessed as benign; and false-positive cases were tumors incorrectly assessed as malignant. The improvement in diagnostic confidence was assessed by receiver operating characteristic curve analysis.[22,23] $P < .05$ was considered significant.

Results

Table 2 shows the different enhancement patterns according to the tumor histotype as reported by the observers involved in the retrospective analysis. The observers did not differ in their classifications of lesion contrast enhancement patterns but exclusively in grading the degree of tumor enhancement.

Table 2. Enhancement Patterns During the Arterial Phase

Histotype	Absent	Dotted	Rimlike	Central	Diffuse
Hepatocellular carcinomas	1	2	0	1	101[a]
Metastases	3	12	13	0	20
Intrahepatic cholangiocarcinomas	1	4	0	0	2
Hemangiomas	1	3	10	0	19[b]
Focal nodular hyperplasia	0	0	0	20[c]	10
Hepatocellular adenomas	0	0	0	0	15
Regenerative nodules	2	8	0	0	9
Focal fatty sparing/changes	1	2	0	2	20
Other benign histotypes[d]	1	0	2	0	1
Total	10	31	25	23	197

Values show the distribution of enhancement patterns observed during the arterial phase according to the histotype, as reported by the readers involved in the retrospective analysis.
[a]In 57 of 101 tumors, the diffuse contrast enhancement appeared homogeneous, whereas it appeared heterogeneous in 44 of 101 tumors. The enhancement pattern was heterogeneous in all hepatocellular carcinomas greater than 3 cm in diameter (n = 55) but only in 15 hepatocellular carcinomas less than 3 cm in diameter.
[b]Diffuse enhancement was observed in 19 liver hemangiomas less than 2 cm.
[c]Central contrast enhancement revealed a spoked wheel shape with central vessel branching toward the tumor periphery. This enhancement pattern was observed in all cases of focal nodular hyperplasia greater than 2 cm in diameter (n = 15) but only in 5 cases of focal nodular hyperplasia 2 cm or less in diameter.
[d]Necrotic nodules revealed absent enhancement; liver abscesses revealed peripheral rimlike enhancement; and intrahepatic extramedullary hematopoiesis revealed homogeneous diffuse enhancement.

Figures 6 and 7 show the distribution of the visual grading for liver tumor enhancement during the arterial and portal and late phases, respectively. Malignant (n = 160) versus benign (n = 126) liver tumors did not differ ($P > .05$) in the degree of contrast enhancement during the arterial phase (Figure 6), with a median grading of +1 versus +1 for all observers. On the other hand, malignant versus benign tumors differed significantly ($P = .001$) in the degree of contrast enhancement during the portal and late phases (Figure 7), with a median grading of –2 or –1 versus 0 or 2 according to the different observers. Malignant tumors exhibiting an atypical isoenhancing appearance in the portal and late phases (n = 38 according to observer 1; n = 27, observer 2; n = 30, observer 3; n = 25, observer 4; n = 8, observer 5; and n = 7, observer 6) corresponded to well-differentiated hepatocellular carcinomas, whereas benign tumors exhibiting an atypical hypoenhancing appearance in the portal and late phases (n = 67 according to observer 1; n = 69, observer 2; n = 48, observer 3; n = 44, observer 4; n = 32, observer 5; and n = 13, observer 6) corresponded to focal nodular hyperplasia, hepatocellular adenomas, and other benign lesions, including thrombotic avascular liver hemangiomas, necrotic nodules, and liver abscesses.

Table 3 shows the level of observer agreement during the different dynamic phases. Observer interpretations were unanimous regarding the

Figure 6. Histograms of the visual grading system for the liver tumor enhancement degree during the arterial phase for the different observers for benign (**A**) and malignant (**B**) tumors. The difference in the enhancement degree between malignant and benign lesions was not significant ($P > .05$, nonparametric Mann-Whitney *U* test).

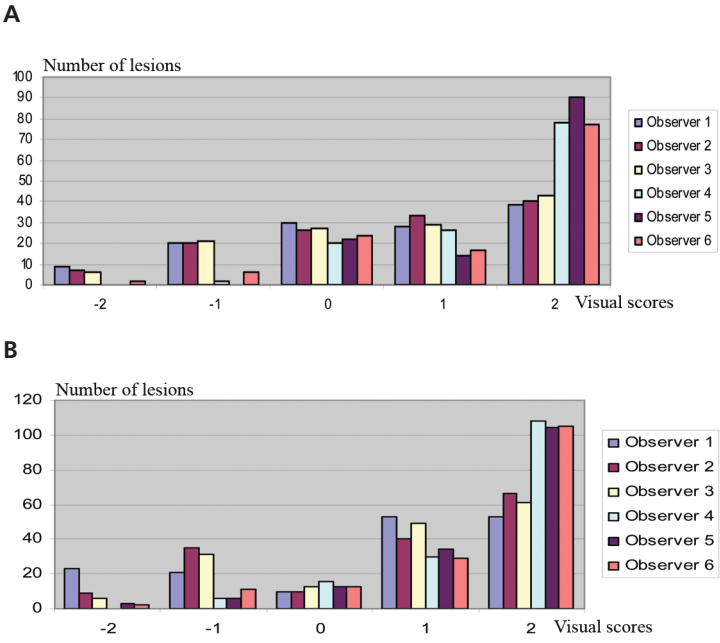

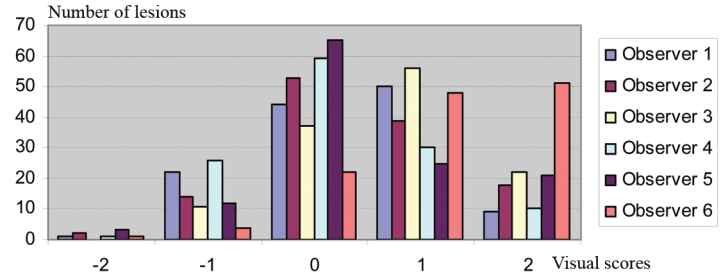

A

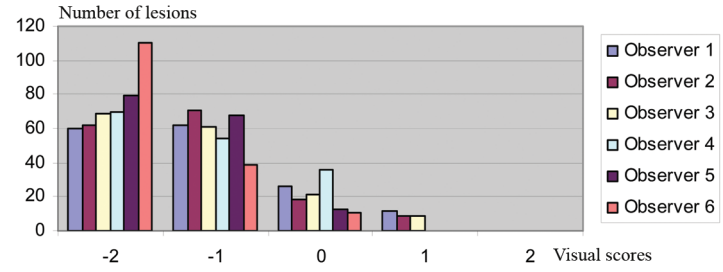

B

Figure 7. Histograms of the visual grading system for the liver tumor enhancement degree during the late phase for the different observers for benign (**A**) and malignant (**B**) tumors. The difference in the enhancement degree between malignant and benign lesions was significant ($P = .001$, nonparametric Mann-Whitney *U* test).

degree of enhancement of most tumors (Figure 8). Interobserver variability occurred for interpretations of tumor enhancement during both the arterial and portal and late phases (Figure 9). Intragroup observer agreement was higher than intergroup agreement in grading tumor enhancement (Table 3). Intragroup observer agreement ($\kappa = 0.63–0.83$) was also higher than intergroup agreement ($\kappa = 0.47–0.63$) in grading diagnostic confidence for liver tumor characterization (Table 4). Greater observer experience provided increased diagnostic performance and confidence (Tables 5 and 6) in malignancy diagnosis. The observers' diagnostic performance and confidence (Tables 5 and 6) in the characterization of liver tumors differed significantly ($P = .01$).

Discussion

Contrast-enhanced ultrasound imaging is a reliable imaging tool in the characterization of liver tumors[9–12] and allows real-time scanning with the possibility of prolonged liver insonation. This has been achieved as a result of the safe profile and stability of microbubbles persisting in the bloodstream for several minutes.[3–5] The operator has to identify the most suitable acoustic window to evaluate the lesion and simply observe tumor enhancement after ultrasound contrast agent injection without moving the transducer from the initial position. Correct image interpretation is less straightforward and depends on the reader's experience, as shown in this study.

In this study, we excluded those liver hemangiomas with a typical enhancement pattern, namely, peripheral nodular enhancement with centripetal fill-in, and those tumors with an overt malignant pattern because their inclusion would have artificially increased the interobserver agreement and would have overestimated the diagnostic capabilities of CEUS. This study included those tumors that could have had variable interpretations of the enhancement degree

Table 3. Interobserver Agreement: Tumor Enhancement Grades

Observer	Observer 1	Observer 2	Observer 3	Observer 4	Observer 5	Observer 6
Arterial phase						
2	0.79					
3	0.77	0.81				
4	0.19	0.22	0.23			
5	0.23	0.25	0.24	0.71		
6	0.26	0.29	0.31	0.62	0.67	
Portal and late phases						
2	0.77					
3	0.63	0.64				
4	0.62	0.51	0.41			
5	0.62	0.64	0.46	0.78		
6	0.48	0.50	0.67	0.54	0.63	

Values are weighted κ statistics for interobserver agreement in assessing the grade of tumoral enhancement during the arterial and portal and late phases.

Figure 8. Unanimous observer interpretations of the degree of tumor enhancement in a 60-year-old man with a regenerative nodule (1 cm in diameter). **A**, Dotted enhancement (arrow) and a hypoenhancing appearance are evident during the arterial phase 30 seconds after ultrasound contrast agent injection. **B**, A hypoenhancing appearance of the lesion (arrow) also persists during the portal phase 70 seconds after contrast agent injection. **C**, The lesion (arrow) has an isoenhancing appearance in comparison with the adjacent liver parenchyma during the late phase 130 seconds after contrast agent injection. All observers classified the tumor as isoenhancing during the late phase and correctly interpreted it as benign.

A

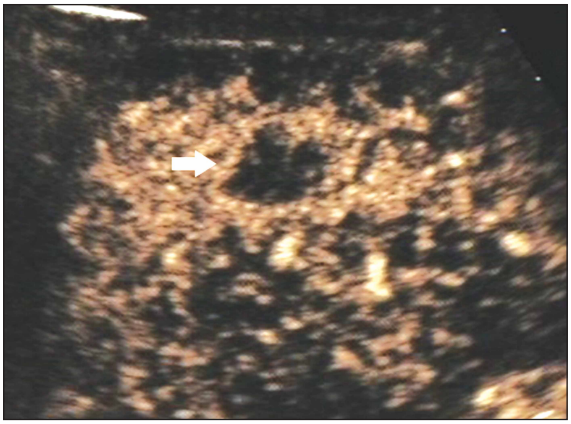

B

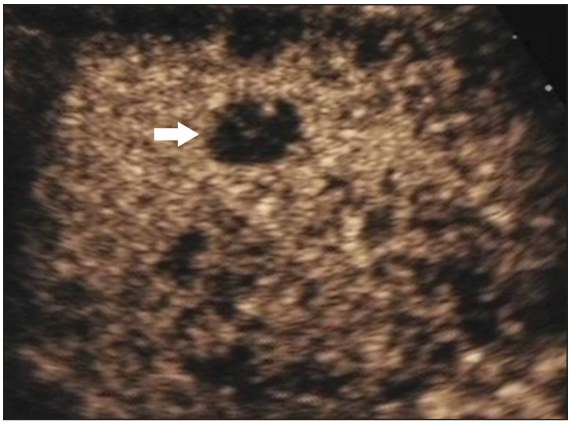

C

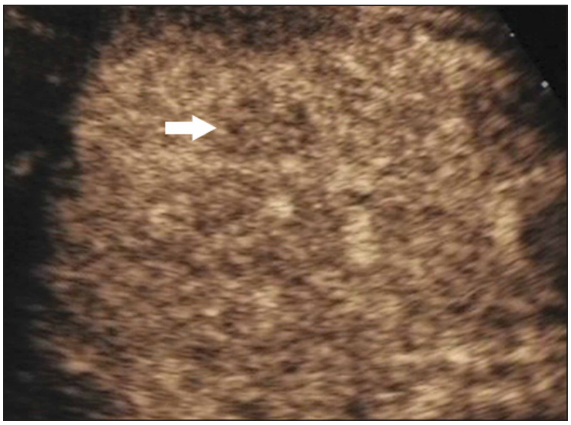

Figure 9. Variability in observer interpretations of the degree of tumor enhancement in a 45-year-old woman with focal nodular hyperplasia (4.5 cm in diameter). **A**, Diffuse homogeneous contrast enhancement (arrow) and a hyperenhancing appearance during the arterial phase 30 seconds after microbubble injection. **B**, The tumor (arrow) has an isoenhancing appearance in comparison with the adjacent liver parenchyma (L) during the portal phase 60 seconds after contrast agent injection. **C**, During the late phase, 140 seconds after contrast agent injection, the same tumor (arrow) shows a nonunivocal enhancement degree in comparison with the adjacent liver parenchyma. Observers 5 and 6 classified the tumor as isoenhancing, whereas the first 4 observers classified the tumor as hypoenhancing, which led to a misclassification of the tumor as malignant.

A

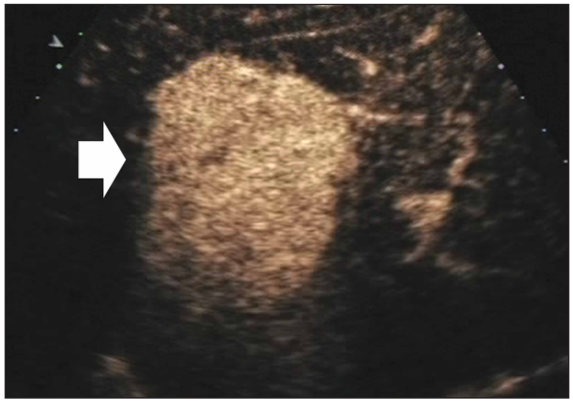

B

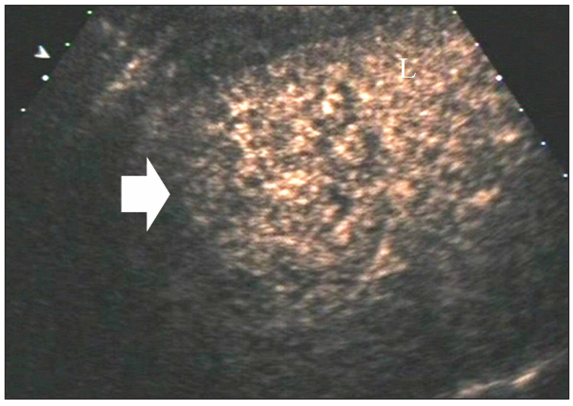

C

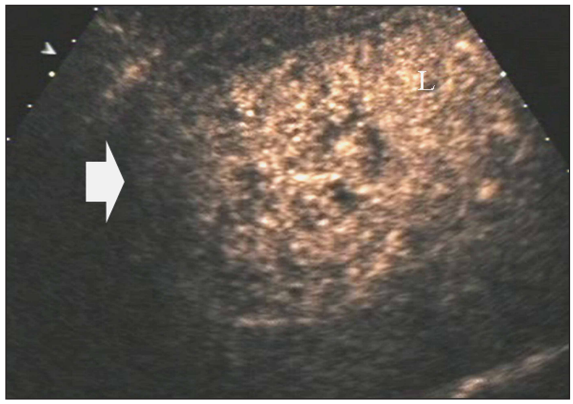

Table 4. Interobserver Agreement: Diagnostic Confidence

Observer	Observer 1	Observer 2	Observer 3	Observer 4	Observer 5	Observer 6
2	0.77					
3	0.63	0.63				
4	0.58	0.50	0.51			
5	0.57	0.60	0.54	0.83		
6	0.47	0.49	0.63	0.63	0.72	

Values are weighted κ statistics for the interobserver level of agreement in grading the diagnostic confidence for liver tumor characterization as benign or malignant.

compared with the adjacent liver for different observers, and we analyzed how this variability could influence the diagnostic performance and confidence of liver tumor characterization on CEUS.

Visual analysis is the simplest method for analyzing liver tumor enhancement. However, visual analysis is often penalized in comparison with quantitative analysis by the fact that the observer's eyes tend to focus on a specific portion of the tumor instead of comparing the echogenicity of the whole tumor and adjacent liver in a more global and reproducible manner. For the purposes of statistical analysis, in this study the different observers were grouped according to the absence (group 1, observers 1–3) or presence (group 2, observers 4–6) of experience in CEUS. Both inexperienced and experienced observers showed good or very good intragroup agreement in assessing the liver tumor degree of enhancement, whereas intergroup agreement was lower. This indicates a clear overlap in the visual analysis provided by the observers with similar levels of experience.

The different gradings of liver tumor enhancement proposed by the observers determined different gradings in diagnostic confidence and, consequently, different values of diagnostic performance according to the observer's experience. Although definite enhancement patterns and degrees of liver tumor enhancement were identified in most of the examined tumors, there was some interobserver variability in the assessment of the liver tumor enhancement degree during both the arterial and portal and late phases, which influenced the correct characterization of liver tumors. Because the diagnostic criteria for liver tumor characterization were based on the enhancement pattern and degree, the better diagnostic performance and confidence shown by the observers with greater experience was related to a more accurate visual assessment of tumor vascularity after microbubble injection and a more effective integration between the tumor enhancement pattern and degree observed during the different dynamic phases.

We identified some overlap between benign and malignant tumors in terms of the degree of tumor enhancement during the portal and late phases due to some benign tumors having a hypoenhancing appearance similar to that of malignancies, as described previously,[10,11,24] and

Table 5. Values of Diagnostic Performance for Each Observer

Observer	Sensitivity	Specificity	Accuracy	PPV	NPV
1	76.2 (122/160)	46.8 (59/126)	63.3 (181/286)	64.5 (122/189)	60.8 (59/97)
2	83.1 (133/160)	45.2 (57/126)	66.4 (190/286)	65.8 (133/202)	67.8 (57/84)
3	81.2 (130/160)	61.9 (78/126)	72.8 (208/286)	73 (130/178)	72.2 (78/108)
4	84.4 (135/160)	65.1 (82/126)	75.9 (217/286)	75.4 (135/179)	76.6 (82/107)
5	95 (152/160)	74.6 (94/126)	86.1 (246/286)	82.6 (152/184)	92.1 (94/102)
6	95.6 (153/160)	89.7 (113/126)	93.1 (266/286)	92.2 (153/166)	94.2 (113/120)

Values indicate diagnostic performance of the different observers involved in the retrospective analysis of the cine clips and are given as percentages and numbers from which the percentages were derived in parentheses. Sensitivity and specificity values were calculated by combining all observers' true- and false-positive results. NPV indicates negative predictive value; and PPV, positive predictive value.

to some hepatocellular carcinomas having an isoenhancing appearance, as do benign tumors. It has already been shown that 50% of hepatocellular carcinomas show typical wash-out by 90 seconds after ultrasound contrast agent injection, whereas in the remaining 50% of cases, contrast wash-out appears after 91 to 180 seconds or even later.[25] The percentages of isoenhancing and hyperenhancing hepatocellular carcinomas in the portal and late phases were also reported to be 33% to 38%.[26,27] This variability may have accounted for some of the interobserver variability found in this study.

Contrast-enhanced ultrasound imaging is technically a simple imaging method and allows real-time acquisition after contrast agent administration without any drawbacks due to an incorrect scanning time in comparison with CT and MRI, which are limited by image acquisition time issues. One limitation of CEUS in comparison with multiphase CT and MRI is the fact that only a single liver tumor can be scanned at a time because the transducer has to be kept still during the examination; furthermore, ultrasound contrast agent injections are necessary to characterize additional liver tumors. Moreover, ultrasound contrast agents are generally safe agents[28] in comparison with iodinated and gadolinium-based contrast agents, which can cause renal or systemic toxicity. On the other hand, CT and MRI allow simultaneous characterization of multiple liver tumors of similar or different natures in the same patient. This is rarely possible with CEUS because the image planes and technical parameters must be individually optimized for each tumor examined. Computed tomography and MRI may, however, be limited in scanning hypervascular tumors, owing to difficulties in starting the acquisition at a suitable time point,[29] and are penalized by costs and patient irradiation.

The main limitation of this study was that we did not evaluate intraobserver variability in differentiating between benign and malignant tumors. In this retrospective study, the ultrasound images were visually interpreted by 6 blinded readers to provide an unbiased analysis of the diagnostic capabilities of CEUS. This does not reflect real routine clinical practice, in which the ultrasound operator usually corresponds to the reader evaluating the ultrasound images. Immediate interpretation of the ultrasound images by the same operator during the routine work flow could further improve the general diagnostic performance of CEUS because the operator is frequently not blinded to the patient's clinical history and other imaging findings.

Table 6. Values of Diagnostic Confidence for Each Observer

Observer	A_z	95% CI
1	0.849	0.805–0.893
2	0.888	0.849–0.926
3	0.918	0.887–0.949
4	0.937	0.911–0.963
5	0.972	0.954–0.990
6	0.989	0.977–1.000

Values indicate the diagnostic confidence of the different observers involved in the retrospective analysis of the cine clips. A_z indicates area under the receiver operating characteristic curve; and CI, confidence interval.

In conclusion, the diagnostic performance of CEUS in liver tumor characterization was dependant on the observer's level of experience.

References

1. Nino Murcia M, Ralls PW, Jeffrey RB Jr, Johnson M. Color flow Doppler characterization of focal hepatic lesions. AJR Am J Roentgenol 1992; 159:1195–1197.
2. Harvey CJ, Albrecht T. Ultrasound of focal liver lesions. Eur Radiol 2001; 11:1578–1593.
3. Schneider M, Arditi M, Barrau MB, et al. BR1: a new ultrasonographic contrast agent based on sulfur hexafluoride-filled microbubbles. Invest Radiol 1995; 30:451–457.
4. Morel DR, Schwieger I, Hohn L, et al. Human pharmacokinetics and safety evaluation of SonoVue, a new contrast agent for ultrasound imaging. Invest Radiol 2000; 35:80–85.
5. Quaia E. Microbubble ultrasound contrast agents: an update. Eur Radiol 2007; 17:1995–2008.
6. Tanaka S, Ioka T, Oshikawa O, Hamada Y, Yoshioka F. Dynamic sonography of hepatic tumors. AJR Am J Roentgenol 2001; 177:799–805.
7. Dill-Macky M, Burns P, Khalili K, Wilson S. Focal hepatic masses: enhancement patterns with SH U 508A and pulse inversion US. Radiology 2002; 222:95–102.
8. Isozaki T, Numata K, Kiba T, et al. Differential diagnosis of hepatic tumors by using contrast enhancement patterns at US. Radiology 2003; 229:798–805.

9. Bryant T, Blomley MJK, Albrecht T, et al. Improved characterization of liver lesions with liver-phase uptake of liver-specific microbubbles: prospective multicenter trials. Radiology 2004; 232:799–809.
10. Wen YL, Kudo M, Zheng RQ, et al. Characterization of hepatic tumors: value of contrast-enhanced coded phase-inversion harmonic angio. AJR Am J Roentgenol 2004; 182:1019–1026.
11. Quaia E, Calliada F, Bertolotto M, et al. Characterization of focal liver lesions by contrast-specific US modes and a sulfur hexafluoride-filled microbubble contrast agent: diagnostic performance and confidence. Radiology 2004; 232:420–430.
12. Burns PN, Wilson SR. Focal liver masses: enhancement patterns on contrast-enhanced images—concordance of US scans with CT scans and MR images. Radiology 2007; 242:162–174.
13. Albrecht T, Blomley M, Bolondi L, et al; EFSUMB Study Group. Guidelines for the use of contrast agents in ultrasound. Ultraschall Med 2004; 25:249–256.
14. Claudon M, Cosgrove D, Albrecht T, et al. Guidelines and good clinical practice recommendations for contrast enhanced ultrasound (CEUS): update 2008. Ultraschall Med 2008; 29:28–44.
15. Xu HX, Liu GJ, Lu MD, et al. Characterization of focal liver lesions using contrast-enhanced sonography with a low mechanical index mode and a sulfur hexafluoride-filled microbubble contrast agent. J Clin Ultrasound 2006; 34: 261–272.
16. Quaia E, Bertolotto M, Dalla Palma L. Characterization of liver hemangiomas with pulse inversion harmonic imaging. Eur Radiol 2002; 12:537–544.
17. Kim TK, Jang HJ, Burns PN, et al. Focal nodular hyperplasia and hepatic adenoma: differentiation with low-mechanical-index contrast-enhanced sonography. AJR Am J Roentgenol 2008; 190:58–66.
18. Nicolau C, Vilana R, Catalá V, et al. Importance of evaluating all vascular phases on contrast-enhanced sonography in the differentiation of benign from malignant focal liver lesions. AJR Am J Roentgenol 2006; 186:158–167.
19. Bismuth H. Surgical anatomy and anatomical surgery of the liver. World J Surg 1982; 6:3–8.
20. Coinaud C. Le Foie: Études Anatomiques et Chirurgicales, Paris, France: Masson; 1957.
21. Kundel HL, Polansky M. Measurement of observer agreement. Radiology 2003; 228:303–308.
22. Beck JR, Shultz EK. The use of relative operating characteristic (ROC) curves in test performance evaluation. Arch Pathol Lab Med 1986; 110:13–20.
23. Hanley JA, McNeil BJ. A method of comparing the areas under receiver operating characteristic curves derived from the same cases. Radiology 1983; 148:839–843.
24. Dietrich CF, Martens JC, Braden B, et al. Contrast-enhanced ultrasound of histologically proven liver hemangiomas. Hepatology 2007; 45:1139–1145.
25. Jang HJ, Kim TK, Burns P, Wilson SR. Enhancement patterns of hepatocellular carcinoma at contrast-enhanced US: comparison with histologic differentiation. Radiology 2007; 244:898–906.
26. Nicolau C, Català V, Vilana R, et al. Evaluation of hepatocellular carcinoma using SonoVue, a second-generation ultrasound contrast agent: correlation with cellular differentiation. Eur Radiol 2004; 14:1092–1099.
27. Quaia E, D'Onofrio M, Cabassa P, et al. Diagnostic value of hepatocellular nodule vascularity after sulfur hexafluoride-filled microbubble injection in patients with liver cirrhosis: analysis of diagnostic performance and confidence in malignancy characterization. AJR Am J Roentgenol 2007; 189:1474–1483.
28. Piscaglia F, Bolondi L; Italian Society for Ultrasound in Medicine and Biology (SIUMB) Study Group on Ultrasound Contrast Agents. The safety of SonoVue in abdominal applications: retrospective analysis of 23,188 investigations. Ultrasound Med Biol 2006; 32:1369–1375.
29. Sultana S, Awai K, Nakayama Y, et al. Hypervascular hepatocellular carcinomas: bolus tracking with a 40-detector CT scanner to time arterial phase imaging. Radiology 2007; 243:140–147.